Online fault tolerance technique for TSV-based 3D-IC

Yi Zhao, Saqib Khursheed, Bashir M. Al-Hashimi *Fellow*, *IEEE*

Abstract—**This paper presents the design, validation and evaluation of an efficient online fault tolerance technique for fault detection and recovery in presence of three TSV defects: voids, delamination between TSV and landing pad, and TSV short-to-substrate. The technique employs transition delay test for TSV fault detection. Fault recovery is achieved by employing redundant TSVs and rerouting signals to fault-free TSVs. This technique is efficient because it requires small (2 x number of TSVs per group) number of clock cycles for fault detection and recovery. Synthesis results using 130-nm design library show that 100% repair capability can be achieved with low area overhead (4% for the best case).**

Index Terms—**Online test, fault tolerance, 3D, TSV, delay test.**

I. INTRODUCTION

Through-Silicon-Vias (TSV) based vertical interconnections is the most popular method for implementing 3D ICs [1]. Recent research has shown that the yield of TSV based 3D-ICs is affected by TSV manufacturing defects [2, 3] and its reliability is affected by thermal stress induced during fabrication process and normal operation [4-6]. TSV manufacturing defects are introduced in the bonding stage of fabrication process when different dies are bonded together and one defective TSV can potentially fail the entire design along with known-good dies. These challenges are highlighted and novel solutions have been proposed for improving testability [7-10], yield and reliability [11-16]. Various types of TSV defects caused by manufacturing process and thermal stress are highlighted in [4, 5]. Out of all these defects, this paper focuses on three TSV defects: void, delamination between TSV and landing pad, and TSV short to substrate, as these have been extensively studied by test community as highlighted by recent literature [7-10]. The electrical models for these defect types are shown in Fig. 1.

One known issue with pre-bond testing is that it does not scale well, because defects can be introduced during bonding stage as well as during normal operation, for example due to thermal stress. Reference [5] shows that thermal stress can damage TSV interconnects, leading to delamination at TSV interface with the bonding pad. Void growth can also occur during normal operation due to thermal load [6]. This motivates the need for improving in-field reliability. A popular method for improving yield is to introduce redundant TSVs and associated control logic [11-16]. References [12-14]

utilized redundant TSVs in a TSV block for improving yield by repairing defective TSVs. Reference [11] employs redundant TSVs (as in [12-14]) and partition multiple regular and redundant TSVs into TSV groups using a grouping ratio, where redundant TSVs are used to repair defective TSVs in a group. This is used to improve yield and reduce hardware overhead. Reference [15] proposed a dedicated switch structure for TSV repair across TSV groups, thus increasing repair efficiency. The only work that focuses on improving in-field TSV reliability is presented in [16], which uses on-chip processor for online fault detection and recovery. The aim of this paper is to present an efficient and cost-effective online fault tolerance technique capable of TSV fault detection and recovery for designs, where such an on-chip processor is not available. The proposed technique is efficient because it provides hardware based solution which requires only 2 clock-cycles for fault detection and recovery per TSV, leading to faster detection and recovery than available methods [15, 16]. It is cost-effective because the hardware overhead is minimized (without affecting repair capability) by selecting the best grouping ratio through an exhaustive search method [11]. Using Synopsys design compiler, it is shown that the hardware overhead of the proposed technique is lower than available techniques [7, 10, 15, 16], while also achieving 100% repair capability.

The rest of the paper is structured as follows: Sec. II briefly describes the electrical models of TSV defects. The proposed online fault tolerance technique is described in Sec. III. Simulation results are presented in Sec. IV and Sec. V concludes the paper.
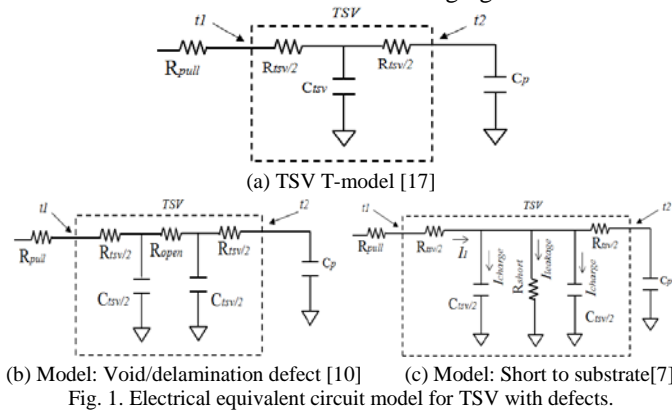
II. PRELIMINARIES

In this work, modelling of TSV is based on a transmission line T-model (Fig. 1(a)) [17], where R_{tsv} and C_{tsv} denote TSV resistance and capacitance respectively, R_{pull} denotes the resistance of the pull-up network of the driving gate and C_p denotes the parasitic capacitance of the circuit. We assume that the signal is transmitted from TSV terminal on die 1 (referred as terminal *t1*) by a driving gate, to the TSV terminal on die 2 (referred as terminal *t2*). Three defects are considered in this work: voids, delamination at interface and short-to-substrate. Void defects are caused by improper TSV filling and thermal stress during normal operation of the device [6]. This defect increases TSV resistance [9] and causes delay faults. Second defect type (TSV delamination defect) is either due to misalignment of bonding pad and TSV during fabrication or due to thermal stress induced on TSV in thermal processing and normal operation. This thermal stress can cause delamination at the interface of TSV structure (TSV and its landing pad) and increases TSV resistance. These two

types of defects (void and delamination) can both be modelled as a resistive open defect, which increases signal delay. The equivalent electrical model of this defect is shown in Fig. 1(b) [10], where a resistor (R_{open}) represents an open defect. Third defect type (short-to-substrate) is due to pinhole in the dielectric layer that is deposited to form the side wall between TSV and substrate. It models a resistive path from TSV to substrate due to the non-conformal sidewall insulation [7]. The electrical equivalent of this defect is shown in Fig. 1(c), in which a short resistor is incorporated, denoted by R_{short}, which represents the leakage current path between TSV and substrate and reduces the current for charging TSV.

(a) TSV T-model [17]

(b) Model: Void/delamination defect [10]   (c) Model: Short to substrate[7]
Fig. 1. Electrical equivalent circuit model for TSV with defects.

III. TSV FAULT TOLERANCE TECHNIQUE

Fig. 2 shows the block diagram of the proposed fault tolerance technique to test and repair a single TSV group with a grouping ratio of 4:2. It consists of three blocks: *detection block*, *recovery block* and *routing block*. These blocks are used to test and repair a group of TSVs (referred as TSV group). A TSV group with a grouping ratio of *m:n*, consists of *m* inputs (output) signals, *m* regular TSVs, and *n* redundant TSVs, where each TSV group can tolerate up to *n* TSV defects. The generic architecture (grouping ratio m:n) is shown in reference [18] (Fig. 8 and associated text) and achieves 100% repair capability as demonstrated in Sec. IV-C of reference [18] (TABLE III and associated text). For illustration, a grouping ratio of *4:2* is shown in Fig. 2. The number of redundant TSVs in a design has an effect on yield, repair capability and hardware cost. For a given fault rate, recent papers have proposed algorithms to determine grouping ratio to minimize hardware cost and maximize yield [11], [15]. In this work, it is assumed that TSVs are divided into groups at design time.

The *detection block* (Fig. 2) is used for testing each TSV in a group. Input test patterns are applied from a die (Die 1) and output test response is observed through Test observation block located on subsequent die (Die 2). A double TSV interconnection is used to update TSV status register on die 1. This concept was also used in [2] for error communication between dies. The detection block uses delay test to differentiate between faulty and fault-free TSVs, where each

TSV is tested for three defect types (Fig. 1). The status of each TSV is updated in TSV status registers, which are located on both dies and holds all locations of faulty TSVs in a group. Note that the detection block does not distinguish between different defect types, as that is typically required for diagnosis. Once fault detection is complete, recovery is initiated to reroute signals through fault-free TSVs (replacing defective TSVs) by reconfiguring the routing block between signals and TSVs (Fig. 2).

Fig. 2. Detection and recovery blocks for a grouping ratio of 4:2
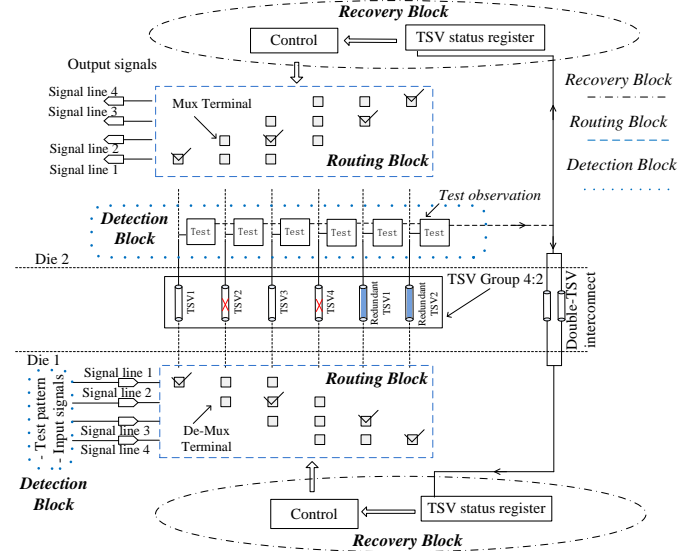
The *recovery block* is implemented on both dies as shown in Fig. 2, and it consists of TSV status register and control. TSV status register holds fault status of each TSV. The control unit provides appropriate control signals for multiplexers inside the Routing block, to connect signal lines with appropriate TSV. The control is also used to report when the number of defective TSVs is higher than the maximum tolerance limit of a TSV group.

The *routing block* consists of a set of multiplexers (for output signals, Die 2) and de-multiplexers (for input signals, Die 1) to connect each signal line to a TSV according to the selection signals provided by the control unit of the Recovery block. The connection boxes (Fig. 2) represent the de-Mux (Mux) terminals for input (output) signal lines. For a grouping ratio of *4:2*, each signal can use one of the three possible TSVs; hence a 1-to-3 de-multiplexer is needed (Fig. 3). Fig. 2 illustrates the detection and recovery blocks for a grouping ratio of 4:2, assuming two defective TSVs (TSV2 and TSV4). See Sec. III of reference [18] for an example that illustrates the working of these three blocks.

A. Detection Block

Fig. 3 shows the detection block for a single TSV, as an example. It consists of an input signal unit for test patterns and input signals, where transition signals are stored for test application. Fig. 3 also shows the test observation block (part
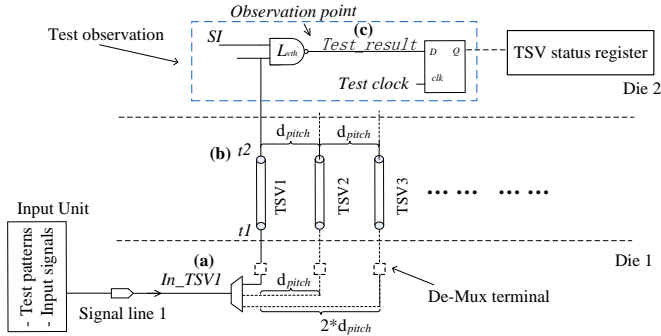
Fig. 3 Detection block for a single TSV

of *Detection block*; Fig. 2), where test output is observed in a flip-flop and stored in TSV status registers. The *SI* signal and NAND gate is used to initialize TSV status registers. The detection block applies a transition signal on a die (Die 1) and the output is observed on the subsequent die (Die 2). We next explain the working of detection block when considering three defects (Fig. 1).

As described in Sec. II, void and delamination defects increase TSV resistance forming a higher resistance TSV path, thus increasing RC delay. To derive RC delay at TSV (*t2*, Fig. 3), we employed TSV electrical model with void or delamination defects (Fig. 1). The RC delay at TSV (*t2*) is:

$$\left(R_{pull} + \frac{1}{2}R_{TSV} + \frac{1}{2}R_{open}\right)C_{TSV} + \left(R_{pull} + R_{TSV} + R_{open}\right)C_p \quad (1)$$

Where, R_{open} denotes the open resistance due to void or delamination defect, R_{pull} denotes the resistance of the pull-up network driving the TSV (de-multiplexers, Fig. 3) and *Cp* denotes the parasitic capacitance of the test circuit. When the TSV is fault-free $R_{open}\sim0$, the TSV resistance is small (in hundreds mΩ) and can be ignored when compared to the pull-up resistance of driving gate R_{pull}, which is usually several kΩ, such that the path delay is not effected by the TSV resistance. However, in case of void or delamination defects, open resistance of a TSV (R_{open}) can be up to 1MΩ [9], which is significantly higher than accumulative effect of R_{TSV} and R_{pull}.

Assuming the NAND gate (Fig. 3) with logic threshold voltage denoted by L_{vth}, where L_{vth} of a gate input is the input voltage at which the output voltage reaches half of the supply voltage, while the other gate input(s) are at non-controlling value(s) [19]. A rising transition is applied to the TSV from *In_TSV1* (Fig. 3), since the delay at t2 end is dependent on the value of R_{open}, the rising transition at *t2* becomes slower, such that at a given capture time, the voltage at the *t2* is lower than L_{vth}, as illustrated in Fig. 4. Therefore, if TSV open resistance due to void or delamination defect exceeds a critical value $R_{open-critical}$, the voltage at *t2* is lower than the L_{vth} at a given signal capture time and therefore the test detects a faulty signal Test_result=1 (Fig. 4). Signal capture time represents the test clock frequency, which is applied to the flip-flop shown in Fig. 3. Note that the internal clock may be used as a test clock to avoid overhead of a separate DFT clock as used in [19]. TSV open critical resistance $R_{open-critical}$ is a function of

logic threshold voltage L_{vth} and signal capture time (denoted by test clock frequency F_{clock}), where L_{vth} is kept at 50% of V_{dd} for illustration, otherwise it varies per gate input and is also effected by process variation [19].

The testing method for short-to-substrate TSV defect is similar to that of void or delamination defects. For short-to-substrate TSV defect, a resistive path between TSV and substrate causes current leakage (Fig. 1(c)), leading to reduced TSV charging current. Assume a rising transition is applied from *In_TSV1* (Fig. 3), which can be expressed as, $I_{charge} = I_1 - I_{leakage}$, where, I_1 is the input current at *t1* and $I_{leakage}$ is the leakage current from TSV to substrate through the short resistor (Fig. 1(c)). Due to lower TSV charging current (I_{charge}), the rising transition time observed at *t2* increases with increase in defect size (Fig. 4). When applying a rising transition signal at *In_TSV1*, TSV with short to substrate defect exhibits degraded voltage level at TSV end (Fig. 4), this is because R_{short} forms a voltage divider between R_{short}, R_{pull} and R_{tsv} (Fig. 1(c)). We have analysed defect behaviour using HSpice and 65-nm design library. It is found that the detection block is capable of detecting all three defects and as expected, detectable defect size increases with test clock frequency. See Sec. IV-A of reference [18] for an illustrative example, which shows characterization of TSV open (short) critical resistance and the increase of detectable resistance range with applied test clock frequency F_{clock}.
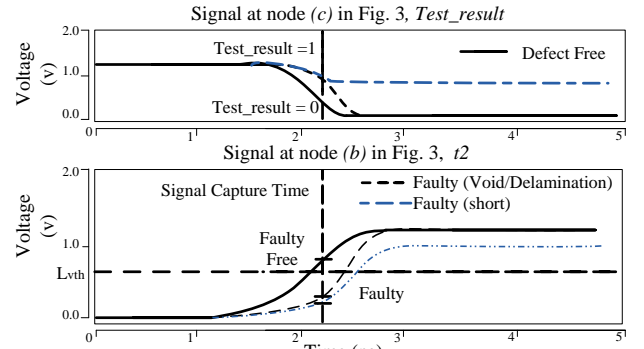

Fig. 4 Test pattern for detection of void or delamination defect

B. Recovery and Routing Blocks

The recovery block (Fig. 2) is used to bypass defective TSVs with fault-free TSVs and it is implemented on both dies that are connected by the TSV group. Recovery is initiated after testing and it is used to reconfigure connections between input/output signals with fault-free TSVs. This section describes the working of reconfiguration process by considering a design with a grouping ratio of *4:2*.

The circuit for reconfiguring input and output signals are similar and therefore only input part is shown in Fig. 5. As can be seen, it consists of the following six components: 1) A routing block consisting of de-multiplexers to connect signal lines with TSVs; 2) A latch chain that controls the de-multiplexers; 3) TSV status register which stores faulty status information for each TSV, where logic '0' indicates fault-free
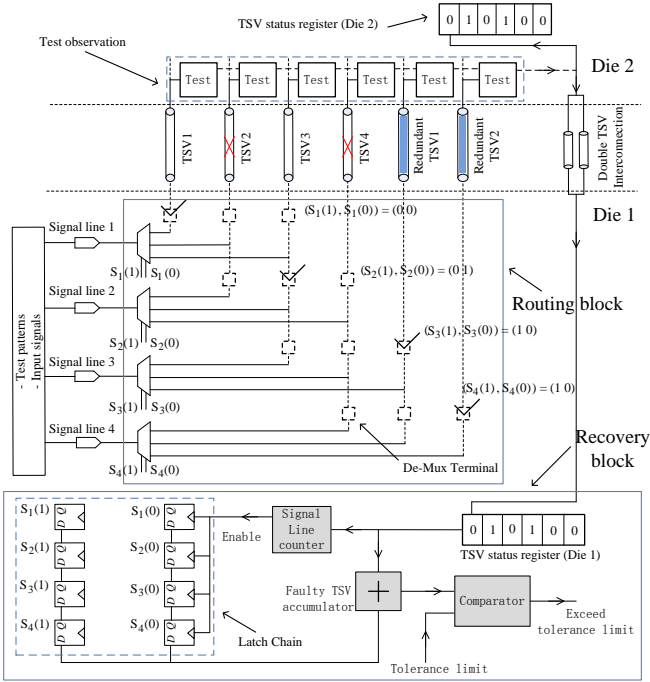
Fig. 5 Reconfiguring a faulty design with a grouping ratio of 4:2

and '1' indicates faulty status of TSV; 4) A signal line counter to indicate the number of signals that have been configured, it is also used to update the latch chain through "enable"; 5) An adder *"Faulty TSV accumulator",* which counts faulty TSV number and provides input to the latch chain; 6) A comparator which compares the existing faulty TSV number with the tolerance limit of the TSV group, and reports an error in case of exceeding the tolerance limit. See Sec. III-B (and Fig. 7(b)) of reference [18] for an illustrative example and a set of test vectors for detecting these defects.

C. Scalability and Hardware Cost

Based on the modelling method for each block this technique can be easily scaled to a design with grouping ratio of m:n. In such configuration each group contains m+n TSVs with m input/output signal lines. The TSV status register consists of m+n bits. Each signal line can have n+1 TSVs for communication, such that 1-to-(n+1) de-multiplexer is needed. Selection signal for signal line i will need $k = \lceil log_2(n+1) \rceil$ bits, which are $S_i(0)$, $S_i(1)$, …, $S_i(k-1)$. Therefore, for each signal line the latch chain consists of k latches, which holds the de-multiplexer selection signal. The signal line counter needs to generate 'm' latch renew enable signals. Overall, for a grouping ratio of m:n, this technique requires m+n clock cycles to test m regular and n redundant TSVs serially and *m+n* clock cycles for repairing all TSVs in the presence of defects. Therefore in total it requires only *2.(m+n)* clock cycles for fault detection and recovery. Theoretical lower bound to test and repair all TSVs per design is 2 clock cycles, assuming the availability of an infrastructure to test and repair all TSV in parallel. The proposed technique approaches

theoretical lower bound by using only *2.(m+n)* clock cycles. See Fig. 8 of reference [18] for the generic architecture. The area overhead of proposed technique (detection, recovery and routing blocks on both dies) is:

$$
\begin{aligned}
Area &= A_{detection} + A_{routing} + A_{recovery} + A_{redundant\ TSV} \\
&= (m+n) \quad Nand\ gates \\
&\quad + \{3(m+n) + 2m\lceil log_2(n+1) \rceil\} \quad FlipFlop \\
&\quad + (m)\ demux_{1-to-(n+1)} + (m)\ mux_{(n+1)-to-1} \\
&\quad + (2)\ signal\ line\ counter_{m-bit} + (2)\ accumulator \\
&\quad + comparator + A_{redundant\ TSV} \quad\quad (2)
\end{aligned}
$$

where "A" denotes area overhead of a TSV group with a grouping ratio of *m:n*; all other notations have their usual meaning. It can be seen that this technique can be easily scaled to suit a generic design with any specified grouping ratio. The wirelength overhead can be understood from Fig. 3, which increases due to alternative route paths from signals to TSVs. For a general grouping ratio of m: n, one signal has *n+1* possible route paths (*n* alternative routes). The lower bound of the wirelength overhead can be achieved based on an assumption that, within a group TSVs are located next to each other with a minimum pitch, denoted as d_{pitch}, and this is applicable to each group (Fig. 3). Such that for *M* total number of signals (*M* regular TSVs) organized with grouping ratio of *m: n*, the wirelength overhead is $M*(\sum_{i=1}^{n} i * d_{pitch})$. This wirelength overhead includes routing block, which dominates the wirelength overhead due to the TSV redundancy. The wirelength overhead due to recovery block is not included in this equation.

IV. SIMULATION RESULTS

Two sets of simulations are conducted to validate and evaluate the fault tolerance technique using STMicroelectronics 130-nm cell library. For validation using HSPICE and ModelSim of the proposed technique, see Sec. IV-A and Sec. IV-B of reference [18].

The cost-effectiveness of this fault tolerance technique is evaluated using five benchmark designs from IWLS 2005 [20]. Table I shows the results in terms of hardware cost of this technique using benchmark designs. The diameter of a TSV is 5-um [17], such that for each redundant TSV, the area overhead is 25 um^2. Regular TSV number for each design is obtained from [21], where selected circuits are synthesised under 130-nm cell library as well. For design with a given number of regular TSVs, the best grouping ratio can be found through an exhaustive search algorithm [11] to minimize area overhead without affecting the targeted repair capability, as shown by the fourth column of Table I. Area overhead of the proposed technique is calculated using Eq. 2 (shown as "calculation" results in Table I) and compared with synthesis results using 130-nm gate library and Synopsys design compiler (Synthesis results, Table I). Area overhead due to each block (Fig. 2) of the proposed fault tolerance technique is shown individually in Table I for calculation results. Synthesis results indicate that area overhead of the proposed technique

is only 4% (best case, *netcard*). Notice this area overhead is due to targeting 100% repair capability, with the expected fault rate of 0.001 (for illustration purposes). See Sec. IV-C of reference [18] for more detail on how 100% repair capability is achieved with selected grouping ratio.

The comparison with recent reported techniques [7, 10, 15, 16] is shown in Table II. For illustration purposes, regular TSV number is assumed to be 1000. In [7, 10] test mechanisms for detecting open TSV defects and short-to-substrate defects are reported. As can be seen (Table I), the proposed technique requires lower area overhead for detection logic when compared with the one reported in [7, 10]. The ideas presented in [15, 16] utilise an on-chip microprocessor to implement control logic for repairing. The proposed work is the first to show detailed hardware solution for designs, where such an on-chip microprocessor is either not employed or cannot be used for TSV repairing.

V. CONCLUSION

This paper has presented a cost-effective and efficient online fault tolerance technique for improving in-field reliability of TSV based 3D ICs. Hardware cost analysis using 130-nm design library shows that 100% repair capability is possible with low area overhead.

ACKNOWLEDGEMENTS

REFERENCES

[1] K. Banerjee *et al*., "3-D ICs: A novel chip design for improving deep-submicrometer interconnect performance and systems-on-chip integration", *Proc. IEEE*, vol. 89, no. 5, pp. 602-633, 2001.
[2] N. Miyakawa *et al*., "Multilayer stacking technology using wafer-to-wafer stacked method," *J. Emerg. Technol. Comput. Syst.* vol. 4, no. 4, 2008.
[3] A. W. T. *et al.*, "Enabling soi based assembly technology for three dimensional integrated circuits," *Electron Devices Meeting, Technical Digest. IEEE Internationa,l (IEDM)*, 2005.
[4] A. D. Trigg, *et al.*, "Design for reliability in via middle and via last 3-D chipstacks incorporating TSVs," *Electronics Packaging Technology Conference (EPTC)*, 2010
[5] L. Gyujei *et al.*, "Interfacial reliability and micropartial stress analysis between TSV and CPB through NIT and MSA," *Electronic Components and Technology Conference (ECTC)*, 2011.
[6] T. Frank *et al.*, "Reliability approach of high density Through Silicon Via (TSV)," *Electronics Packaging Technology Conference (EPTC)*, 2010.
[7] Minki Cho *et al.*, "Design method and test structure to characterize and repair TSV defect induced signal degradation in 3D system," *Computer-Aided Design (ICCAD)*, pp.694-697, Nov. 2010.

[8] Po-Yuan Chen *et al.*, "On-Chip TSV Testing for 3D IC before Bonding Using Sense Amplification," *Asian Test Symposium,* pp.450-455, Nov. 2009.
[9] Shi-Yu Huang *et al.*, "Small delay testing for TSVs in 3-D ICs," *Design Automation Conference (DAC)*, 2012.
[10] Ye Fangming and K. Chakrabarty, "TSV open defects in 3D integrated circuits: Characterization, test, and optimal spare allocation," *Design Automation Conference (DAC)*, 2012.
[11] Y. Zhao, *et al.*, "Cost-Effective TSV Grouping for Yield Improvement of 3D-ICs", *Asian Test Symposium (ATS)*, Nov 2011.
[12] I. Loi *et al.*, "A low-overhead fault tolerance scheme for TSV-based 3-D network on chip links", *International Conference on Computer-Aided Design (ICCAD)*, 2008.
[13] U. Kang, *et al.* "8Gb 3-D DDR3 DRAM using through-silicon-via technology". *IEEE Journal of Solid-State Circuits*, 45(1):111–119, 2010
[14] A.-C. Hsieh *et al.*, "TSV Redundancy: Architecture and Design Issues in 3D IC," pp. 166-171, *Design, Automation & Test in Europe (DATE)*, 2010.
[15] L. Jiang *et al.*, "On effective TSV repair for 3D-stacked ICs," *DATE,* pp.793-798, *Design, Automation & Test in Europe (DATE)*, 2012.
[16] L. Jiang *et al.* "On effective and efficient in-field TSV repair for stacked 3D ICs", *Design Automation Conference (DAC)*, 2013.
[17] G. Katti *et al.*, "Electrical Modeling and Characterization of Through Silicon via for Three-Dimensional ICs," *Electron Devices, IEEE Transactions on*, vol.57, no.1, pp.256-262, Jan 2010.
[18] Y. Zhao, "Design and Validation of Online Fault Tolerance Architecture for TSV-based 3D-IC," *Technical Report*-URL: http://eprints.soton.ac.uk/id/eprint/362558.
[19] S. Khursheed *et al.*, "Delay Test for Diagnosis of Power Switches," *IEEE Trans. on Very Large Scale Integration (VLSI) Systems,*2013.
[20] IWLS 2005 Benchmark circuits.-URL: http://iwls.org/iwls2005/benchmarks.html
[21] J. Cong *et al.*, "Thermal-aware cell and through-silicon-via co-placement for 3D ICs", *Design Automation Conference (DAC)*, pp.670-675, 2011.

TABLE II: Comparison between proposed technique and [7, 10, 15, 16] (regular TSV number is 1000)

Technique		Proposed technique	TSV repairing [15, 16]	Test method	
				[7]	[10]
Objective		Detection (open and short to substrate defect) and Repairing	Repairing	Detection (short to substrate)	Detection (open)
Cost	No. redundant TSV	25 (grouping ratio 80:2)	128	N/A	N/A
	Routing	1000 Mux	3000 Mux	N/A	N/A
	Recovery	13*Signal line counter +13*Faulty TSV adder +13*comp+3025*FF	On-chip microprocessor + Router configuration block	N/A	N/A
	Detection (testing logic)	1025*Nand + 1025*FF	On-chip test block	1k*Voltage comp + 2k*INV+ 1k*FF+ 2k*Mux	1k*voltage comp + 1k*INV+ 1k*FF+ 1k*Mux

TABLE I: Area overhead analysis of the proposed fault tolerance technique (TSV failure rate 0.001).

Circuits	Design area (um^2)	regular TSV (signal TSV)	best grouping ratio [11]	No. of Spare TSV	Area Overhead per die (calculation) /um^2							Synthesis results /um^2	
					Spare TSV area	DoubleTSV structure	Detection	Recovery	Routing	Total (calculation)	Overall percentage (calculation)	Total (synthesis)	Overall percentage (synthesis)
aes_core	818,750	1,362	80:2	34	850	850	16,857	81,832	28,874	129,264	15.79%	143,007	17.4%
ethernet	2,858,975	3,782	80:2	94	2,350	2,350	46,809	227,232	80,178	358,920	12.55%	397,080	13.8%
des_perf	3,428,571	3,678	80:2	92	2,300	2,300	45,522	220,983	77,974	349,079	10.18%	386,190	11.2%
vga_lcd	4,400,000	7,356	240:3	93	2,325	1,550	89,934	408,738	252,311	754,857	17.16%	828,748	18.8%
netcard	28,034,722	9112	240:3	114	2,850	1,900	111,403	506,310	312,542	935,005	3.34%	1,133,868	4.0%